FTIR and Solid State ^{13}C NMR Studies on the Interaction of Lithium Cations with Polyether Poly(urethane urea)

Hsing-Lung Wang,[†] Hsien-Ming Kao,[‡] Mohanlal Digar,[†] and Ten-Chin Wen*[,†]

Department of Chemical Engineering, National Cheng Kung University, Tainan 701, Taiwan; and Department of Chemistry, National Central University, Chung-Li, Taiwan 32054

Received June 26, 2000

ABSTRACT: The behaviors of lithium ions in a polyether poly(urethane urea) (PEUU) were investigated by differential scanning calorimetry (DSC), Fourier transform infrared (FTIR) spectroscopy, ac impedance and ^{13}C magic angle spinning (MAS) solid-state NMR measurements. The PEUU used in this study is composed of poly(ethylene glycol) (PEG, mol wt 1000) as the soft segment and 4,4′-methylenebis(cyclohexyl isocyanate) extended with ethylenediamine (EDA) as the hard segment. The results of DSC measurements indicate the formation of transient cross-links between Li^+ ions and the ether oxygens on complexation with $LiClO_4$, resulting in an increase in the soft segment T_g. A detailed analysis of −NH stretching regions shows an appreciable shift in the free as well as the hydrogen-bonded −NH stretching bands, suggesting possible interactions of Li^+ ions with both hard and soft segments of PEUU. The Arrhenius-like behavior of ionic conductivity with reciprocal temperature implies an activated hopping mechanism for transport of the charge carriers where the charge carriers are decoupled from the segmental motion of the polymer chains. Moreover, significant line broadening, slight upfield chemical shift, and short T_{CH}, observed in the ^{13}C NMR spectra for the carbons attached to the ether oxygens as the dopant was added into the polymer, indicate a coordination between the Li cation and the ether oxygens in the soft segments.

Introduction

Since the discovery of ionic conductivity in some polyether-based polymer hosts complexed with alkali metal salts by Wright et al.[1,2] in 1973, significant advances have been made in the material characteristics and also in the structure of these polymer−salt complexes. Recognizing that the ionic conductivity of polymer electrolytes is facilitated in the elastomeric amorphous phase by the segmental motion of the polymer chains, significant research effort has been devoted in tailoring a polymer structure having a highly flexible backbone and amorphous character. This has led to the discovery of poly[bis(methoxyethoxyethoxide)phosphezene] (MEEP), the Li salt complexes of which are fully amorphous and exhibit a conductivity of $\sim 2 \times 10^{-5}$ S/cm at room temperature, which is one of the highest among the conventional polymer electrolytes.[3] However, the dimensional stability of these polymers is among the poorest. It is not possible to use most of the MEEP/Li salt complexes as separators in batteries since the polymer and the Li salt complexes are glutinous materials having a tendency to flow even under mild pressure at ambient temperature.[4]

Linear segmented polyurethanes are $(A-B)_n$ type copolymers comprised of alternating sequences of glassy or hard (A) material and a rubbery or soft (B) material. The unfavorable interactions between the hard and soft segments make the system a microphase-separated one, which imparts elastomeric properties to polyurethane. The primary driving force for phase separation is the strong intermolecular interaction of the urethane units, which are capable of forming inter urethane hydrogen bonds. Because of such interactions, interconnected or isolated hard segments remain distributed in the soft segment matrix, though the soft phase may contain some hard segments dissolved in it, which is evident from the hydrogen bonding of the urethane −NH groups with the oxygen of the ether or ester linkages.[5,6] Because of this unique two-phase microstructure, the segmented polyurethanes find themselves very much useful as matrix materials for polymer electrolytes. The rubbery soft segments can dissolve alkali metal salts without formation of ionic clusters, which may be due to the interaction of the ether oxygens with the alkali metal ions.[7,8] Furthermore, the low glass transition temperature (T_g) and hence higher segmental motion of these soft segments leads to higher mobility of the dissolved ions. The ability of the soft segments to dissolve alkali metal ions along with higher ionic mobility results in a relatively high ionic conductivity. On the other hand, the hard segment domains, which are in the glassy state and are either distributed or interconnected throughout the rubbery phase, act as reinforcing filler and hence contribute to the dimensional stability of the polymer electrolytes.

Several researchers[9−16] have investigated the morphology and conductivity of thermoplastic polyurethane (TPU) based electrolytes having different hard and soft segments using methods such as DSC, FTIR, ac impedance measurements, Raman spectroscopy, etc. Watanabe et al.[11,12] investigated the correlation between conductivity and morphology of a 4,4′-methylenebis(phenyl isocyanate)/poly(propylene oxide)/ethylenediamine (MDI/PPO/EDA) based PEUU complexed with $LiClO_4$ by means of DSC and dynamic mechanical thermal analysis (DMTA). $LiClO_4$ can be selectively dissolved in the PPO soft phase, and hence, the T_g of the soft segment increases with $LiClO_4$ concentrations. The temperature dependence of ionic conductivity has been interpreted with an equation that is a superposition of Williams−Landel−Ferry (WLF) type equation

* Corresponding author. Telephone: 886-6-2385487. Fax: 886-6-2344496. E-mail: tcwen@mail.ncku.edu.tw.
[†] National Cheng Kung University.
[‡] National Central University.

10.1021/ma001096k CCC: $20.00
Published on Web 01/03/2001

for ionic mobility and Arrhenius equation for the numbers of charge carriers. van Heumen et al.[14] reported the change in morphology of a 4,4′-methylenebis(phenyl isocyanate)/poly(tetramethylene oxide)/1,4-butanediol (MDI/PTMO/BDO) based TPU as a function of salt concentration. An interaction of the lithium cations within the hard segment and between the hard and soft phases has been suggested above a critical salt concentration of 0.5 mmol/g of TPU. As a result of this interaction, the characteristic phase-segregated morphology of TPU is changed to a new one, which improved the thermal stability of the system over the undoped TPU. Recently we found a partial phase mixing of IPDI/PPO-based WPU electrolytes doped with $LiClO_4$ by means of FTIR, XPS, and DSC studies.[16] A saturation level of $LiClO_4$ has been observed between 1 and 2 mmol of $LiClO_4$/g of WPU concentrations. Samples containing higher amounts of salt than the saturation level were found to follow the Arrhenius relationship, whereas the samples containing the salt lower than the saturation level follows Vogel−Tamman−Fulcher (VTF) equation.

In the past few years, solid state NMR has emerged as one of the highly sophisticated techniques used to investigate the ionic structure and mobility of the charge carriers and also to gain insight into the polymer−salt interactions in the polymer electrolytes.[17−30] In particular, the NMR relaxation times depend on the time modulation of the local interactions (e.g., chemical shielding, dipolar, quadrupolar) which indirectly reflects the motions of the nucleus. The different relaxation times are sensitive to different parts of the frequency spectrum of the fluctuations. For example, the mobility of the cation and the segmental motions of the polymer backbone in the megahertz and kilohertz ranges can be obtained by means of spin−lattice relaxation times in the laboratory frame and the rotating frame (i.e., T_1 and $T_{1\rho}$), respectively. Forsyth et al.[23] reported the effect of plasticizer addition on the ionic structure and mobility in a sodium triflate/PEUU solid polymer electrolyte by using ^{23}Na and ^{19}F NMR spectroscopy. Addition of plasticizers results in upfield chemical shifts for the ^{23}Na resonance as a consequence of a decreased ion association and an increased cation−plasticizer interaction. Ward et al.[20] investigated the mobility of the ions and also the effect of these ions on the chain mobility of the PEO polymer matrix doped with $LiCF_3SO_3$ by measuring ^7Li and ^{19}F self-diffusion constants. Stallworth et al.,[21] from their work on PMMA-based gel electrolyte system doped with $LiClO_4$, $LiPF_6$, and $LiN(CF_3SO_2)_2$, reported a significantly different immediate environment for both the cations and anions in gel and liquid electrolytes. Recently, Ng et al.[28] investigated a urethane cross-linked PEG polymer doped with $LiClO_4$ and $LiCF_3SO_3$ by DMTA and solid-state NMR measurements and indicated, from their ^7Li spin−lattice relaxation time (T_1) measurements, that the cationic environment was similar regardless of the nature of the anion. A shift in the mechanism of ion mobility has been suggested, where Li ions are transmitted between aggregates and hence is less influenced by the segmental motion of the polymer chains. In early ^7Li NMR relaxation studies, different ^7Li sites could not usually be resolved, and consequently, differences in their mobilities were detected via the relaxation time measurements. In our previous communication,[31] we reported, for the first time, the presence of at least two distinct Li^+ sites in a 4,4′-methylenebis(cyclohexyl isocyanate)/poly(ethylene oxide)/ethylenediamine (H_{12}MDI/PEO/EDA) PEUU system doped with $LiClO_4$ by measuring ^7Li NMR spectra under conditions of magic angle spinning (MAS) and high-power proton decoupling. In this paper, a detailed ^{13}C MAS NMR study has been conducted along with DSC, FTIR, and ac impedance measurements to investigate the effects of salt concentration and temperature on the phase morphology and bulk impedance of the same PEUU system doped with different amounts of $LiClO_4$.

Experimental Section

Synthesis of PEUU. Poly(ethylene glycol) (PEG; Showa; $M_w = 1000$) was dried and degassed under vacuum at 85 °C for at least 1 day. All other reagents and chemicals were reagent grade and used without further treatment.

The PEUU was synthesized by a two-step addition reaction in a 2.0 L four-necked round-bottom flask equipped with an anchor-propeller stirrer, a nitrogen inlet and outlet, and a thermocouple connected to the temperature controller. In a typical reaction PEG (100 g, 0.1 mol) and 4,4′-methylenebis(cyclohexyl isocyanate) (H_{12}MDI; Aldrich) (81.33 g, 0.31 mol) were simultaneously added to the reactor previously flashed with dry nitrogen gas, to form a prepolymer of PEUU. The temperature was kept at 50 °C initially. After proper mixing (100 rpm), two drops of di-*n*-butyltin(IV) dilaurate (DBTDL) were added into the batch to catalyze the reaction, and then the temperature was slowly raised to 85 °C. After 6 h of reaction at this temperature, ~700 g of dimethylformamide (DMF; Tedia) was added to the prepolymer to dissolve it completely. Then the chain extender, ethylenediamine (EDA; Merck) (12.6 g, 0.21 mol) which was previously diluted to a 10% solution in DMF, was added slowly to convert the prepolymer into polymer. After the addition of the chain extender is finished, the chain extension reaction was allowed to continue for 1 h more, and then a few drops of methyl alcohol were added to terminate the reaction.

Determination of Molecular Weight of PEUU. Molecule weight of the synthesized PEUU has been determined using a Shimadzn gel permeation chromatograph (GPC) connected to a Shimadzn HPLC pump and an RI detector. 1% solution of the PEUU in DMF was injected into the GPC column (Jordi Gel DVB mixed bed) at a flow rate of 2 mL/min. The number-average molecular weight and the polydispersity index of the PEUU are 282 000 and 3.59, respectively.

Solution NMR Experiments. High-resolution NMR measurements were performed on a Bruker AMX-400 spectrometer with ^1H and ^{13}C resonance frequencies at 400.13 and 100.61 MHz, respectively. The PEUU sample was dissolved in deuterated dimethyl sulfoxide (DMSO-d_6). ^1H and ^{13}C chemical shifts are referenced relative to tetramethylsilane (TMS) at 0.0 ppm.

Preparation of Polymer Films. A 10 mass % sample of the PEUU solution was mixed well with a 10 mass % solution of lithium perchlorate ($LiClO_4$, Aldrich) dissolved in DMF in various proportion to make polymer electrolytes with different concentration of $LiClO_4$. The mixed solution was cast onto polypropylene plates and the solvent was slowly removed under vacuum at 50 °C for 7 days. The films were then stored in an argon filled drybox (Vacuum Atmospheres Co.) for further measurements. The thicknesses of the films were controlled to be in the range of 100−150 μm.

DSC Thermograms. Thermal analysis of the polymer electrolytes was carried out in a DuPont DSC 2010 differential scanning calorimeter with a heating rate of 10 °C/min and over the temperature range −100 to +120 °C. Polymer electrolyte films were sealed in aluminum capsules and transferred out of the drybox to perform thermal analysis. Glass transition temperatures (T_g) were reported as the midpoint of the transition process. All the thermograms were baseline corrected and calibrated against indium metal.

FTIR Spectroscopy. Films for infrared analysis were prepared by casting 5 mass % DMF solutions onto potassium

Table 1. Thermal Transition Temperatures for Lithium Salt Doped PEUUs

[$LiClO_4$(mmol/g of PEUU)	T_g (°C)	$\Delta T_g/\Delta C$ ((°C/mmol)/g of PEUU)
0.0	-43.9	-
0.1	-41.4	25
0.5	-22.8	42
1.0	-20.9	22
1.5	-17.9	17

bromide windows at room temperature. After the majority of the solvent was evaporated, the films were placed in a vacuum oven at about 80 °C for over 48 h to remove residual solvent and moisture. FTIR spectra were measured at ambient temperature using a Nicolet 550 instrument with a wavenumber resolution of 2 cm^{-1}. Band deconvolution of the resulting spectra was obtained by analysis with Grams 386 software (Galatic). In most cases the deconvolution was conducted several times to examine alternate deconvolutions and hence to obtain the best fit for the same band envelope.

Impedance Spectroscopy. The ionic conductivity of the polymer electrolytes was obtained via impedance analysis with an electrochemical cell consisting of the electrolyte film sandwiched between two blocks of stainless steel, sealed with an O-ring in a double wall glass tube through the outer jacket of which thermostated water was circulated for measurements at different temperatures. The temperature of the cell was controlled using a water thermostat (HAAKE D8 & G) calibrated against a Pt resistance thermometer. The impedance analysis was performed by using a frequency response analyzer (Eco Chemie B. V.) with an Autolab FRA2 modulus under an oscillation potential of 10 mV from 1 MHz to 1 Hz.

Solid-State NMR Measurements. Solid-state ^{13}C magic angle spinning (MAS) NMR experiments were performed on a Bruker AVANCE−400 spectrometer, equipped with a Bruker double-tuned 7 mm probe, with resonance frequencies of 100.6 MHz for ^{13}C nuclei. The Hartmann−Hahn condition for $^1H \rightarrow {}^{13}C$ cross-polarization (CP) experiments was determined using admantane. The $\pi/2$ pulse lengths for ^1H and ^{13}C were typically 4 and 6 μs, respectively. A repetition time of 4 s was used. The^{13}C chemical shifts were externally referenced to tetramethylsilane (TMS). The $^1H \rightarrow {}^{13}C$ CP spectra were recorded as a function of contact time using a single-contact pulse sequence with reversal of spin temperature in the rotating frame and with high-power proton decoupling during the ^{13}C signal acquisition. This pulse sequence was used for ordinary CP experiments as well as for the proton and carbon spin−lattice relaxation measurements in the rotating frame (i.e., $T_{1\rho}^H$ and $T_{1\rho}^C$).

Results and Discussion

DSC. As the hard and soft segments of PEUUs are thermodynamically incompatible, separate thermal transitions are visible for both the hard and soft segments. In polyether urethane, the soft segment T_g is observed in the negative temperature region whereas, depending upon the amount of hard segment, multiple thermal transitions are observed in the region of 70 to above 200 °C. Solvation of alkali metal salts by polyethers has been reported to occur by means of coordination of the alkali metal cations with the ether oxygen of the polyethers. Many researchers[9−16] have studied the effect of such coordination on the soft segment T_g of TPUs. The results of our thermal measurements are presented in Table 1, where the soft segment T_g is found to increase as the salt concentration is increased. This is consistent with previous investigations of $LiClO_4$-doped TPUs containing either PEO[9,10] or PPO[11,12] as the soft segment. It is also similar to the T_g results of polyether complexes with $LiCF_3SO_3$.[14] It is clear that in this study the lithium cation is stabilized by the PEG soft segment via the formation of transient cross-links, leading to an increase in the soft-segment T_g. By normalization of the T_g data against salt concentration, $\Delta T_g/\Delta C$ was calculated and also listed in Table 1. An examination of $\Delta T_g/\Delta C$ values indicates a nonlinear increase with the increasing $LiClO_4$ concentration. The value of $\Delta T_g/\Delta C$ decreases as the salt concentration is increased (Table 1). This may be attributed to the plasticizing effect from the formation of charge-neutral contact ion pairs with increasing salt concentrations.[14] The neutral contact ion pairs lose the ability to provide ionic cross-links; hence, the further increase in T_g is not significant.

Table 2. Deconvolution Results of the FTIR Spectra in the −NH Stretching Region

	peak position (cm^{-1})			
film	1	2	3	4
PEUU0.0	3510	3384	3308	3260
PEUU0.5	3520	3406	3355	3284
PEUU1.0	3531	3415	3364	3291
PEUU1.5	3535	3443	3379	3300
	peak area (%)[a]			
film	1	2	3	4
PEUU0.0	36.8	17.1	26.8	19.3
PEUU0.5	35.0	13.5	19.6	31.9
PEUU1.0	35.7	10.9	20.9	32.5
PEUU1.5	33.3	9.8	18.7	38.2

[a] The peak areas are based on total N−H stretching band area.

FTIR Analysis. FTIR has been employed to investigate the effect of salt concentration on the phase morphology of the PEUU electrolytes. The −NH stretching region (3050−3700 cm^{-1}) of the FTIR spectra has been considered for this purpose. Deconvolution of the −NH stretching region to the best fits (Gaussian line) results four different peaks. The deconvolution results of all the samples are presented in Table 2 and the corresponding deconvoluted spectra in the −NH stretching region are shown in Figure 1. As reported by others,[32−34] peaks 1, 3, and 4 can be assigned to the three characteristic bands for −NH stretching vibrations. Peak 1, in the region 3510−3535 cm^{-1} is assigned to the free −NH stretching vibration. Peak 3 in the region 3305−3380 cm^{-1} is assigned to the −NH groups H-bonded to the carbonyl oxygen of the hard segment while peak 4 in the region 3260−3300 cm^{-1} is assigned to the −NH groups H-bonded to the ether oxygen of the soft segment. Peak 2 in the region 3380−3445 cm^{-1} can be assigned as the overtone to the fundamental in the carbonyl region.[14]

An examination of Table 2 and Figure 1 indicates significant changes of the −NH stretching vibrations due to complexation with Li salt. All the three −NH peaks are shifted to higher frequency with addition of $LiClO_4$. Variation of the N−H bond strength as a result of change in extent of H-bonding due to complexation with Li^+ ions is responsible for such shifting of the peak positions. Table 2 also shows the variation of percent area of each of the bands with salt concentration. Each of the band areas was normalized on the basis of the total −NH stretching band area. Quantitative estimation of the free and H-bonded −NH groups from the band areas may lead to erroneous results, as the absorptivity coefficient for the H-bonded −NH band is a function of the strength of the H-bond and the band frequency.[32,34] It is evident from Table 2 that the frequency shift is more in the case of H-bonded −NH

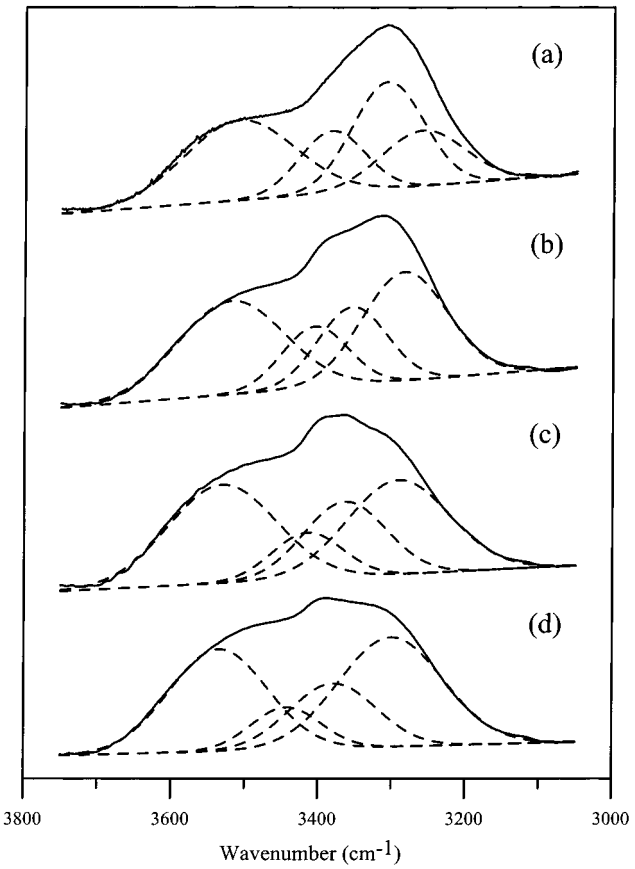

Figure 1. Decomposition of N−H stretching region for PEUU doped with vaious $LiClO_4$ concentrations: (a) 0, (b) 0.5, (c) 1.0, and (d) 1.5 mmol/g of PEUU.

Scheme 1. Schematic Representation of Coordination of Li^+ Ions to Different Positions: (a) to the Nitrogen Atoms of Free − NH Groups, (b) to the Hydrogen-Bonded Carbonyl Oxygens, and (c) to the Hydrogen-Bonded Ether Oxygens

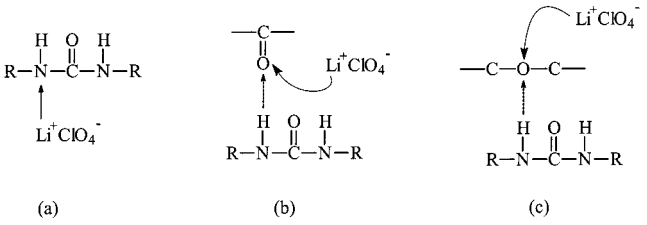

bands rather than the free −NH band. As reported by Ferry et al.,[15] this may be due to the competition of Li^+ ions' coordination with H-bonding. Coordination of Li^+ ions to different positions of PEUU is shown in Scheme 1. Scheme 1a indicates the interaction of the Li^+ ions with the N atoms of free −NH groups. Interaction between the Li^+ ions and the lone pair of electrons on the nitrogen atom[35] leads to reduction of the N−H bond length, and hence the band position for peak 1 shifts to higher frequency. Shifting of the band position for peak 3 can be explained with the help of Scheme 1b where the Li^+ ions are coordinated with the carbonyl oxygens H-bonded to −NH groups. As band position is related to the strength of the H-bonded N−H bond, the shift to higher frequency with increasing salt concentration indicated an increase in the bond strength of the N−H bond. This is likely due to the localization of the electrons of the H-bonded carbonyl oxygens through coordination of the Li^+ cations (Scheme 1b). Thus, the strength of the hydrogen bonding between −NH and

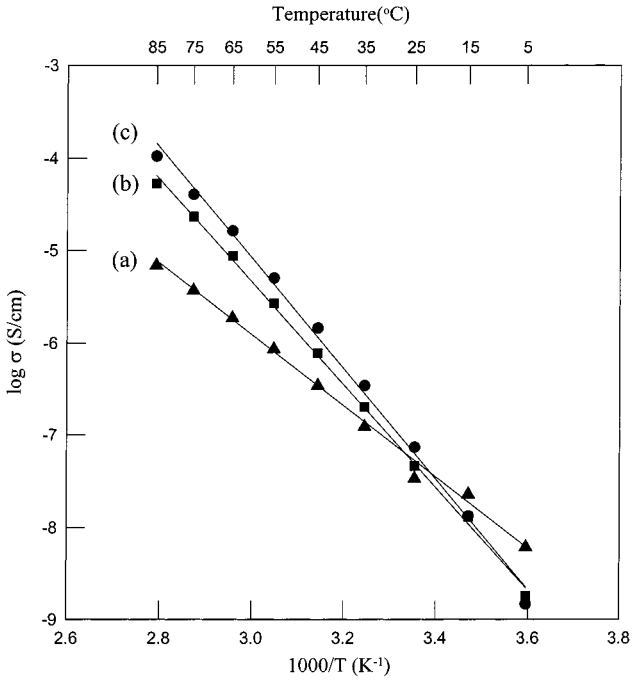

Figure 2. Dependence of conductivity on the reciprocal of temperature for PEUU doped with various $LiClO_4$ concentrations: (a) 0.5, (b) 1.0, and (c) 1.5 mmol/g of PEUU.

carbonyls is weakened, resulting in the shift of −NH band to higher frequency. Besides, the band position of peak 4 also shifts to higher frequency with increase in salt concentration. This may be due to the coordination of nonbonded electrons of ether oxygens by the Li^+ ions, leading to weakening of the H-bond strength between −NH and −O− groups (Scheme 1c). This will result in a consequent increase in N−H bond strength, and hence, the band position will be shifted to higher frequency.

As has been mentioned earlier, the interaction of Li^+ ions is more with the H-bonded sites rather than the free −NH groups. This is evident from the frequency shift of the −NH peaks with salt concentration. In the case of free −NH groups, 25 cm^{-1} shifting was observed for doping with 1.5 mmol $LiClO_4$/g PEUU, whereas the H-bonded peaks (peaks 3 and 4) shift by 71 and 40 cm^{-1} respectively. The comparatively higher shifting of peak 3 indicates that the Li^+ ions coordinate preferentially to the hard segment carbonyl oxygens, which is also reported by other researches.[15] The expected change of the peak 4 band position is due to the well-known coordination of Li^+ ions to the ether oxygens of the soft segment. Such interaction of the Li^+ ions with the soft segment is also evident from the DSC and NMR studies. From DSC studies, the soft-segment T_g was found to increase with salt concentration. The interaction of the Li^+ ions with the hard and soft segments will be discussed in more detail in the NMR part of this paper.

Ac Impedance. The ionic conductivity of polyether urethane based polymer electrolyte systems has been reported earlier by many researchers.[9−16] Variation of conductivity with temperature was found to follow either a VTF (eq 1) or an Arrhenius (eq 2) relationship, depending upon whether the ion mobility is coupled with the segmental motion of the polymer chains,

$$\sigma = AT^{-1/2} \exp\left(\frac{-B}{k_B(T - T_0)}\right) \qquad (1)$$

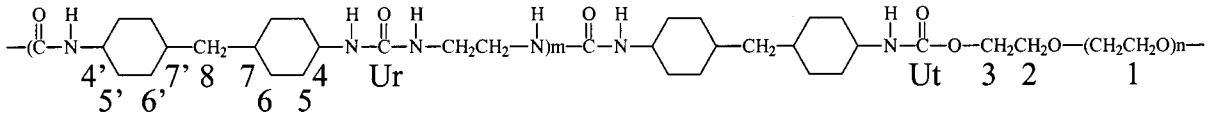

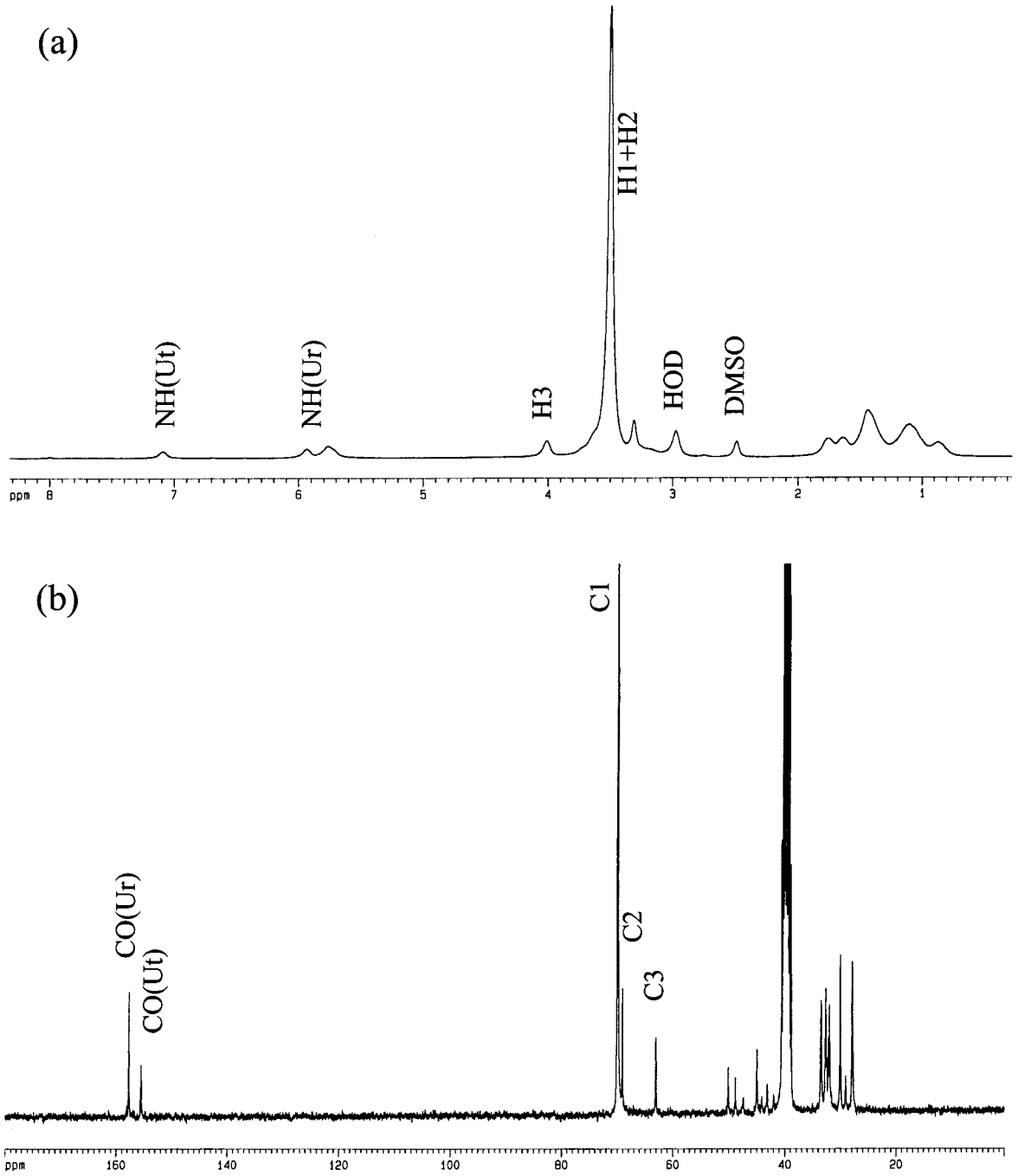

Figure 3. (a) ^{1}H and (b) ^{13}C high-resolution solution NMR spectra and the structure of the repeat unit for the pure PEUU (top).

$$\sigma = A \exp\left(\frac{-E}{k_B T}\right) \qquad (2)$$

where A is a constant proportional to the number of carrier ions, B is the pseudoactivation energy related to polymer segmental motion, k_B is the Boltzmann constant, E is the activation energy, and T_0 is a reference temperature usually associated with the ideal T_g at which free volume disappears or the temperature at which the configurational entropy becomes zero.

Application of the VTF relationship for ion transport requires the coupling of the charge carriers with the segmental motion of the polymer chains. On the other hand, the Arrhenius relationship is applicable when the ions are decoupled from the polymer host. For the later case, ion movement occurs by activated hopping. In Figure 2, the ionic conductivity data for the electrolyte samples are presented against reciprocal temperature.

Table 3. Assignments of ^{1}H and ^{13}C Solution NMR Chemical Shifts of PEUU, Where the Structure of the Repeat Unit is Shown as Above

chem shift (ppm)	assignment[a]	chem shift (ppm)	assignment
	(a) ^{1}H NMR Data		
7.09	NH(Ut)	3.10	HOD
5.93	NH(Ur)	2.97	H9
5.76		2.49	DMSO-d_6
4.00	H3	1.75−0.87	H4 + H5 + H6 + H7 + H4′ + H5′ + H6′ + H7′ + H8
3.49	H1 + H2		
	(b) ^{13}C NMR Data		
69.94	C1	155.46	CO(Ut)
69.06	C2	157.67	CO(Ur)
63.02	C3	40.53	C9
33.5−27.7	C5 + C6 + C8 + C5′ + C6′	39.70	DMSO-d_6
50.1−44.0	C4 + C7 + C4′ + C7′		

[a] Remarks: Ut = urethane; Ur = urea.

It is evident from Figure 2 that the temperature dependency of the conductivity data follows the Arrhenius equation. This indicates that the charge carriers are decoupled from the segmental motion of the polymer chain and transport occurs via an activated hopping mechanism. As is evident from Figure 2, the relationship between conductivity and salt concentration is a complex one. At lower temperature regions higher salt containing electrolytes have lower conductivity, whereas at higher temperature region the reverse relationship was observed. Samples containing higher amount of salt improve conductivity by increasing the number of charge carriers, but the T_g of the polymer is also simultaneously increased, which decreases the ionic mobility. Hence, in the lower temperature region, the samples containing a higher amount of the salt, though containing increased number of charge carriers, show lower conductivities as the mobility is restricted due to the higher T_g of the soft segment. Another possibility is the increase in ion pair formation with increasing salt concentration.[36] Moreover, as evidenced from the FTIR and NMR results some of the Li^+ ions may be coordinated to the hard segment urethane and/or urea groups and hence will not contribute to conductivity unless the temperature region close to the hard segment T_g is reached.

Calculation of activation energies from the slope of the curves in Figure 2 gives values of 73.92, 106.54, and 114.50 kJ/mol for samples containing 0.5, 1.0, and 1.5 mmol of $LiClO_4$/g of PEUU, respectively. This indicates that the activation energy is increased with increasing salt concentration, which is not unlikely because the ionic mobility is decreased as T_g is increased with salt concentration. Higher T_g produces free volume at a particular temperature and hence lesser ionic diffusivity.

Identification of the Structure of PEUU by ^{1}H and ^{13}C Solution NMR. The ^{1}H and ^{13}C solution NMR spectra of PEUU in DMSO-d_6 at room temperature are shown in Figure 3. The chemical shift assignments are listed in Table 3. There exist two kinds of −NH groups in the polymer: one is in the urethane unit and the other is in the urea unit. The ^{1}H peaks at 5.93 and 5.76 ppm are assigned to the −NH group of the urea unit, based on the *J*-coupling splitting. The downfield 7.09 ppm is assigned to the −NH group in the urethane unit since the −NH group is attached to a carboxylic group. The ^{13}C peaks appearing at 157.67 and 155.46 ppm are assigned to the carbonyl carbons in the urea and urethane groups, respectively.

^{13}C CP/MAS NMR. Figure 4a shows the ^{13}C CP/MAS NMR spectrum, acquired at room temperature, of the pure PEUU. A broad peak centered at 159.0 ppm and a shoulder at 155.5 ppm (see inset), are observed in the carbonyl region and are assigned to the urea and urethane carbons, respectively. The resonance at 71 ppm is assigned to those soft-segment carbons that are adjacent to oxygen, while the small resonance around 65 ppm is ascribed to the soft-segment carbons that are adjacent to a urethane linkage. The peaks at 50 and 41 ppm are attributed to the secondary carbons on the cyclohexyl rings bonded to the nitrogen atoms and the CH_2 groups (C8), respectively. The peak at 33 ppm is associated with the primary carbons in the cyclohexyl rings (cf. Table 3). It is interesting to note that the line width of the 71 ppm peak is remarkably sharp as compared with other peaks. This feature implies that an effective motional narrowing undergoes possibly due to the segmental motion of the polymer chain. The above peak assignment is based on the ^{1}H and ^{13}C solution NMR spectra (Figure 3 and Table 3).

For comparison, Figure 4b displays the ^{13}C CP/MAS spectrum of the PEUU doped with $LiClO_4$ (1.5 mmol/g). Upon the addition of $LiClO_4$, the spectral resolution for the urethane and urea carbons in the carbonyl region degrades and their respective peaks cannot be resolved. Moreover, significant line broadening is observed with the peak at 71 ppm (see inset) as the salt is added. For example, the full width at half-maximum (fwhm) of the 71 ppm peak is 77 Hz without the dopant, and gradually increases with the increasing salt concentrations, and becomes 350 Hz for the 1.5 mmol/g of $LiClO_4$/PEUU sample (see inset for comparison). This broadening indicates that the presence of Li salts causes a more broad distribution of the soft-segment environments and/or reduces the segmental motion; the latter results from the electronic interaction between the Li^+ cations and the ether oxygen atoms in the soft-segments. Thus, a broader peak is observed when the dopant exists. Similar behavior has been observed in ionic conducting polymers.[37] In addition, the chemical shifts at 159 and 71 ppm shift upfield slightly by addition of $LiClO_4$. The small ^{13}C chemical shift change is also due to the interactions of the Li^+ cation with the polymer chains. Such upfield ^{13}C chemical shifts have been correlated to the oxygen−cation interactions for poly(ethylene oxide) (PEO) and crown ether salt complexes.[38,39] On the other hand, the ^{13}C chemical shifts and the line widths for other carbons are not very sensitive to the presence of the dopant.

To gain more insight into the influence of Li^+ ions on the polymer chain dynamics, ^{1}H → ^{13}C CP experiments have been performed as a function of contact time, ranging from 0.1 to 20 ms. The T_{CH} and $T_{1\rho}^H$ measurements were obtained by fitting the CP signal intensities with the following formula:[40]

$$M(t) = M_0 \exp(-t/T_{1\rho}^H)(1 - \exp(-t/T_{CH})) \qquad (3)$$

where $M(t)$ is the peak intensity as a function of contact time t, M_0 is the normalization constant; $T_{1\rho}^H$ is the proton spin−lattice relaxation time in the rotating frame, and T_{CH} is the cross-polarization constant. Figure

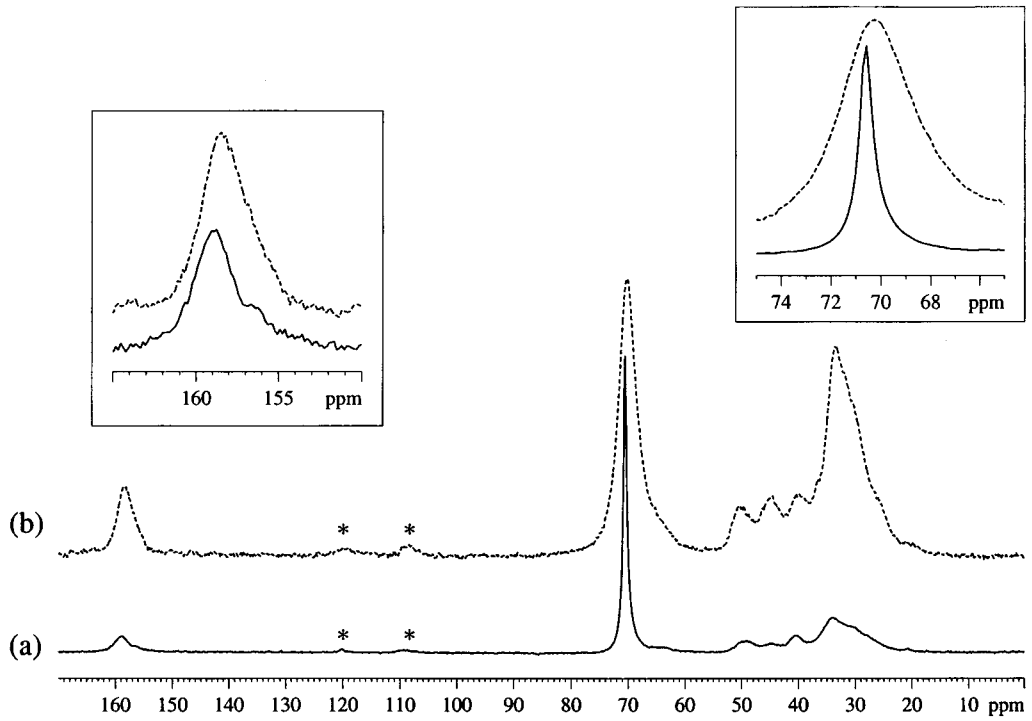

Figure 4. ^{13}C CP/MAS spectra for the PEUU (a) undoped and (b) doped with 1.5 mmol/g of $LiClO_4$ acquired at room temperature and at a spinning speed of 5 kHz. Asterisks denote spinning sidebands. The carbonyl and ether carbon regions are enlarged as shown in the insets.

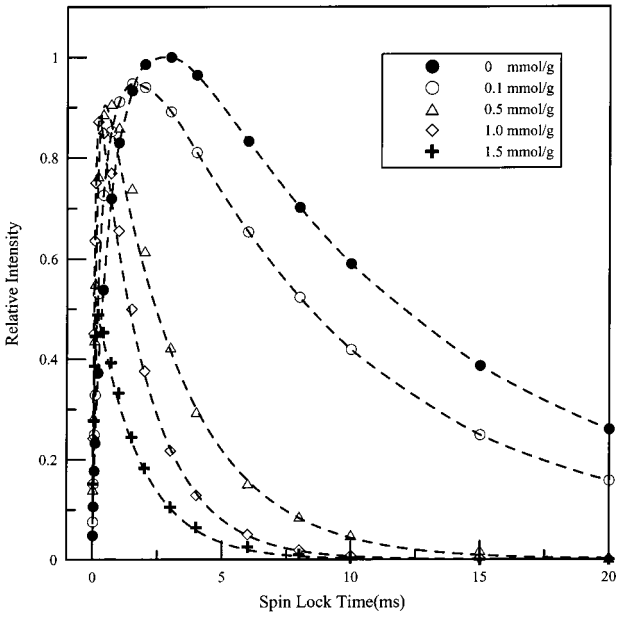

Figure 5. Evolution of $^1H \rightarrow {}^{13}C$ CP signal intensities for the 71 ppm peak (ether carbon) as a function of the contact time with various $LiClO_4$ concentrations. The dashed lines are calculated using eq 3 with the parameters in Table 4.

5 shows the $^1H \rightarrow {}^{13}C$ CP intensities for the ether carbons at different doping levels as a function of contact time. The results of the contact time measurements for the peaks at 159, 71, and 33 ppm are presented in Table 4. Without adding the Li salts, the soft-segment peak at 71 ppm and the hard-segment peak at 33 ppm exhibit T_{CH} values of 0.6 and 0.03 ms and $T_{1\rho}^H$ values of 11.6 and 2.13 ms, respectively. The slower growth in spin magnetization for the soft-segment peak at 71 ppm, compared with that of the hard-segment peak at 33 ppm (both have two protons attached), is consistent with the higher mobility of the soft-phase carbons. This reflects

Table 4. T_{CH} and $T_{1\rho}^H$ As Determined from Variable Contact Time NMR Experiments

carbon	chem shift (ppm)	lithium salt concn (mmol/g)	T_{CH} (ms)	$T_{1\rho}^H$ (ms)
primary carbons in the cyclohexyl rings	33	0	0.031	2.127
		0.1	0.032	2.462
		0.5	0.032	2.319
		1.0	0.033	2.618
		1.5	0.038	2.604
soft-segment carbons adjacent to oxygen	71	0	0.558	11.603
		0.1	0.318	10.801
		0.5	0.141	2.971
		1.0	0.070	1.956
		1.5	0.057	1.795
H_{12}MDI urea carbonyl	159	0	0.306	2.817
		0.1	0.319	2.757
		0.5	0.311	2.470
		1.0	0.338	2.337
		1.5	0.373	2.212

that the rapid motion of the soft-segment carbons makes the CP signal transfer from the proton spins less efficient than for the hard-segment carbons. As seen in Table 4, there is a gradual decrease in T_{CH} as the salt concentration is increased. The significant decrease in T_{CH} for the peak at 71 ppm with the addition of salt suggests a possible coordination of Li^+ ions with the ether oxygen atoms of the polymer chain, thereby restricting the segmental motion of the soft segments. However, it is to be noted that the variation of T_{CH} is not linear with salt concentrations, which indicates the possibility of formation of contact ion pairs at higher salt concentrations. Being neutral in nature, the ion pairs cannot coordinate with the ether oxygen atoms, and hence the decrease in T_{CH} at higher salt concentration is not significant.

Surprisingly, the contact time experiments for the urethane and urea carbonyls were found to fit with single-component exponential. This implies that these

Table 5. ^{13}C $T_{1\rho}^{C}$ Relaxation Times and Relative Fractions

carbon	chem shift (ppm)	lithium salt concn (mmol/g)	$T_{1\rho}^{C}$ fast component %	fast component ms	slow component %	slow component ms
primary carbons in the cyclohexyl rings	33	0	46	1.006	54	4.314
		0.1	44	1.020	56	4.693
		0.5	45	0.972	55	4.306
		1.0	50	1.259	50	5.488
		1.5	44	1.196	56	4.583
soft-segment carbons adjacent to oxygen	71	0	50	3.438	50	13.796
		0.1	52	2.661	48	10.726
		0.5	61	1.424	39	4.087
		1.0	62	1.090	38	2.962
		1.5	64	1.006	36	2.604
H_{12}MDI urea carbonyl	159	0			100	29.796
		0.1			100	28.204
		0.5			100	27.119
		1.0			100	26.853
		1.5			100	23.182

two carbonyls have similar T_{CH} and $T_{1\rho}^{H}$ values after salt doping. However, a slight increase in T_{CH} is observed with the increasing in Li salts. This implies that the original H-bonding network involved in the urethane and urea units between polymer chains might be partly destroyed upon the addition of Li salts (see Scheme 1b). This effect increases the mobility of urethane and urea units, and therefore raising their T_{CH} values due to the poorer CP efficiency. However, this effect is not significant. Because of the poor resolution in the carbonyl region for the urethane and urea carbons, it is not possible to differentiate their respective relaxation times, and this will not be discussed further.

As seen in Table 4, it is also clear that there are distinct protons spin reservoirs coupled to the different carbons, suggesting proton spin diffusion is relatively slow due to the phase separation in PEUU. The $T_{1\rho}^{H}$ value for the protons associated with the soft segment suddenly drops as the salt concentration is 0.5 mmol/g, reflecting that proton−proton spin diffusion become more efficient due to the increased proton−proton dipolar interaction. This observation indicates that the coordination between Li^+ ions and the soft segments in the polymer chains effectively reduces the chain motion, resulting in the increase in the chain rigidity, and therefore increases proton−proton dipolar interaction.

^{13}C spin−lattice relaxation times in the rotating frame ($T_{1\rho}^{C}$) have previously been shown to be sensitive to molecular motions in polymers with frequencies in the range of tens of kilohertz.[41−43] Recently, Root et al. demonstrated that $T_{1\rho}^{C}$ relaxation measurements was the most useful for the class of polymers exhibiting microphase separation such as a poly(urethane urea) system.[44] $T_{1\rho}^{C}$ measurements were performed by using a variable-length spin-locking ^{13}C pulse following a standard CP sequence to generate ^{13}C magnetization. The relaxation data shown in Table 5 were obtained using a two-component model as shown below:

$$M(t) = M_A \exp(-t/T_{1\rho A}) + M_B \exp(-t/T_{1\rho B}) \quad (4)$$

where M_A and M_B are the equilibrium magnetizations and $T_{1\rho A}$ and $T_{1\rho B}$ are the carbon spin−lattice relaxation time constants in the rotating frame for components A and B. The relaxation plot for the ether carbons in the segments with various salt concentrations is shown in Figure 6. The use of two components to fit the relaxation data indicates that there is morphological heterogeneity.

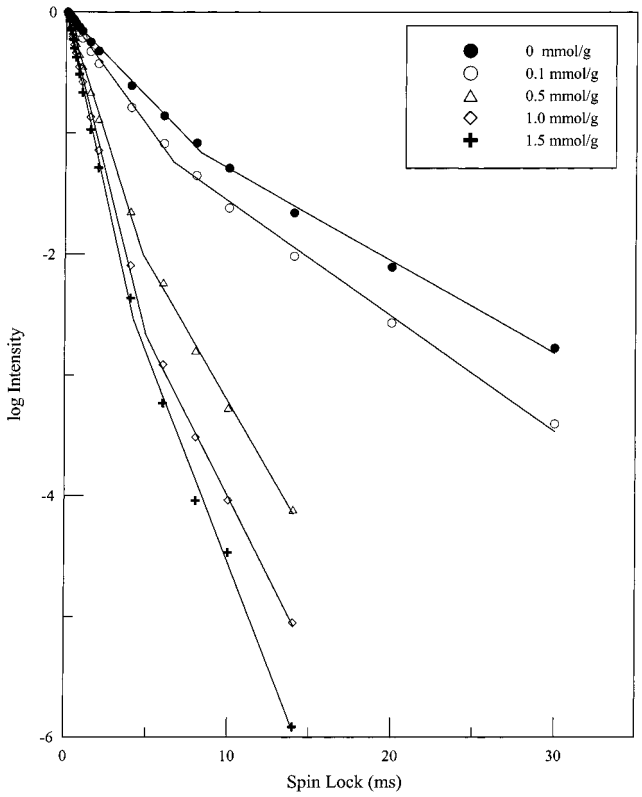

Figure 6. ^{13}C $T_{1\rho}^{C}$ relaxation plots for the 71 ppm peak (ether carbon) for PEUU doped with various $LiClO_4$ concentrations.

The fast and slow components could respond with soft segments that are adjacent to the hard and soft segments, respectively.[44] As seen from Table 5, the $T_{1\rho}^{C}$ values of the two components for the 71 ppm peak decrease with the increasing salt concentrations; the slow component decreases dramatically compared with the fast component, and the $T_{1\rho}^{C}$ values of the two components become very close at high salt concentration. It indicates that the mobility of fast and slow components become similar, compared with that of PEUU without dopant. This observation is possibly due to the miscibility enhancement between the polymer chains at higher salt concentrations. Rapid $T_{1\rho}^{C}$ relaxation occurring in the ether carbon for both the components, compared with the hard-segment carbons, implies that there is a substantial degree of motion near the ^{13}C spin-locking pulse field strength (45 kHz) at high salt concentrations. Very similar values were found from the same experiments carried out at different radio frequency field strength; this means that the condition $\omega_1\tau_c \ll 1$ holds true for the motions involved.[45] Since the motional narrowing condition ($\omega_1\tau_c \ll 1$) is satisfied for the ether carbons at room temperature, the observation of the decrease in $T_{1\rho}^{C}$ following the addition of salt can be explained with a reduced mobility in the kHz region. Moreover, the population of the fast component relative to that of the slow component increases as the salt concentration is increased, implying a phase mixing between soft and hard segments.

In contrast to the ether carbon, the urethane and urea carbons exhibit longer $T_{1\rho}^{C}$ values, consistent with the slowly relaxing characteristics of the hard domains. It appears that the $T_{1\rho}^{C}$ relaxation of the 159 ppm peak due to the urethane and urea carbons can be described adequately by a single-component decay, with a time

constant in the range 23−30 ms. Their $T_{1\rho}^{C}$ values also decrease as the salt concentration is increased. This observation can be explained by Scheme 1a: the addition of salts weakens interchain H-bonding between the hard segments. Since the peaks of the urethane and urea carbons cannot be resolved, a clear and definite conclusion from relaxation analysis for morphology cannot be made. As shown in Table 5, there is no significant change in the relative populations and the relaxation times between fast and slow components for the peak at 33 ppm with the increasing salt concentrations, indicating the Li cation is not in close proximity to the cyclohexyl rings.

Conclusions

A polymer electrolyte based on PEUU complexed with $LiClO_4$ shows significant interaction of Li^+ ions with the soft and hard segments of PEUU. As a consequence of this interaction, there is a change in the two-phase microstructure of PEUU, which is evident from the increase in T_g of the soft segments and the shifting of the H-bonded −NH bands to higher frequency. The ^{13}C CP/MAS NMR analyses also show significant difference in the molecular dynamics of the soft segments when complexed with $LiClO_4$. The decrease in the line width and T_{CH} for the ether carbons in the soft segment indicates a possible coordination of Li^+ ions with the soft segment. Ionic conductivity data ($\sim 10^{-5}-10^{-4}$ S/cm at 85 °C) indicate that the PEUU−$LiClO_4$ system can be used as polymer electrolyte where high conductivity and dimensional stability are required at high temperature.

Acknowledgment. The financial support of this work by the National Science Council of Taiwan under Grants NSC88-2622-E006-008 and NSC89-2214-E006-012 is gratefully acknowledged. The authors highly appreciated Ms. Ru-Rong Wu for her profound contribution in NMR experiments.

References and Notes

(1) Fenton, B. E.; Parker, J. M.; Wright, P. V. *Polymer* **1973**, *14*, 589.
(2) Wright, P. V. *Br. Polym. J.* **1975**, *7*, 319.
(3) Blonsky, P. M.; Shriver, D. F.; Austin, P.; Allcock, H. R. *J. Am. Chem. Soc.* **1984**, *106*, 6854.
(4) Abraham, K. M. In *Application of Electroactive Polymers*; Scrosati, B., Ed.; Chapman and Hall: London, 1993; p 87.
(5) Srichatrapimuk, V. W.; Cooper, S. L. *J. Macromol. Sci.—Phys.* **1978**, *B15*, 267.
(6) Senich, G. A.; MacKnight, W. J. *Macromolecules* **1980**, *13*, 106.
(7) Mocanin, J.; Cuddihy, E. F. *J. Polym. Sci. C* **1966**, *14*, 313.
(8) Santaniello, E.; Manzocchi, A.; Sozzani, P. *Tetrahedron Lett.* **1979**, *47*, 4581.
(9) McLennaghan, A. W.; Pethrick, R. A. *Eur. Polym. J.* **1988**, *24*, 1063.
(10) McLennaghan, A. W.; Hooper, A.; Pethrick, R. A. *Eur. Polym. J.* **1989**, *25*, 1297.
(11) Watanabe, M.; Oohashi, S.; Sanui, K.; Ogata, N.; Kobayashi, T.; Ohtaki, Z. *Macromolecules* **1985**, *18*, 1945.
(12) Watanabe, M.; Sanui, K.; Ogata, N. *Macromolecules* **1986**, *19*, 815.
(13) Seki, M.; Sato, K. *Makromol. Chem.* **1992**, *193*, 2971.
(14) van Heumen, J. D.; Stevens, J. R. *Macromolecules* **1995,** *28*, 4268.
(15) Ferry, A.; Jacobsson, P.; van Heumen, J. D.; Stevens, J. R. *Polymer* **1996**, *37*, 737.
(16) Wen, T. C.; Wu, M. S.; Yang, C. H. *Macromolecules* **1999**, *32*, 2712.
(17) Kim, C. H.; Park, J. K.; Kim, W. J. *Solid State Ionics* **1999**, *116*, 53.
(18) Mustarelli, P.; Quartarone, E.; Capiglia, C.; Tomasi, C.; Magistris, A. *Solid State Ionics* **1999**, *122*, 285.
(19) Ali, F.; Forsyth, M.; Garcia, M. C.; Smith, M. E.; Strange, J. H. *Solid State Nucl. Magn. Reson.* **1995**, *5*, 217.
(20) Ward, I. M.; Boden, N.; Cruickshank, J.; Leng, S. A. *Electrochim. Acta* **1995**, *40*, 2071.
(21) Stallworth, P. E.; Greenbaum, S. G.; Croce, F.; Slane, S.; Salomon, M. *Electrochim. Acta* **1995**, *40*, 2137.
(22) Forsyth, M.; Meakin, P. M.; MacFarlane, D. R. *Electrochim. Acta* **1995**, *40*, 2339.
(23) Forsyth, M.; MacFarlane, D. R.; Meakin, P.; Smith, M. E.; Bastow, T. J. *Electrochim. Acta* **1995**, *40*, 2343.
(24) Forsyth, M.; Garcia, M.; MacFarlane, D. R.; Meakin, P.; Ng, S.; Smith, M. E. *Solid State Ionics* **1996**, *85*, 209.
(25) Shan, W.; Zax, D. B. *Electrochim. Acta* **1997**, *42*, 3513.
(26) Williamson, M. J.; Southall, J. P.; Hubbard, H. V. St. A.; Johnston, S. F.; Davies, G. R.; Ward, I. M. *Electrochim. Acta* **1998**, *43*, 1415.
(27) Ferry, A.; Oradd, G.; Jacobsson, P. *Electrochim. Acta* **1998**, *43*, 1471.
(28) Ng, S. T. C.; Forsyth, M.; MacFarlane, D. R.; Garcia, M.; Smith, M. E.; Strange, J. H. *Polymer* **1998**, *39*, 6261.
(29) Forsyth, M.; Jiazeng, S.; MacFarlane, D. R. *Electrochim. Acta* **2000**, *45*, 1237.
(30) Forsyth, M.; MacFarlane, D. R.; Hill, A. J. *Electrochim. Acta* **2000**, *45*, 1243.
(31) Wang, H. L.; Kao, H. M.; Wen, T. C. Submitted to *Macromolecules*.
(32) Coleman, M. M.; Lee, K. H.; Skrovanek, D. J.; Painter, P. C. *Macromolecules* **1986**, *19*, 2149.
(33) Coleman, M. M.; Skrovanek, D. J.; Howe, S. E.; Painter, P. C. *Macromolecules* **1985**, *18*, 299.
(34) Lee, H. S.; Wang, Y. K.; Hsu, S. L.; *Macromolecules* **1987**, *20*, 2089.
(35) Lu, X.; Weiss, R. A. *Macromolecules* **1991**, *24*, 4381.
(36) Schantz, S.; Torell, L. M.; Stevens, J. R. *J. Chem. Phys.* **1991**, *94*, 6862.
(37) O′Gara, J. F.; Nazri, G.; MacArthur, K. M. *Solid State Ionics* **1991**, *47*, 87−96.
(38) (a) Ibemisi, J. A.; Kimsinger, J. B. *J. Polym. Sci. Polym. Chem. Ed.* **1980**, *18*, 1123−1126. (b) Bekturov, E. A.; Kudaibergenov, S. E.; Bakanova, Z. K.; Vshamov, V. Z.; Kanapyanova, G. S. *Polym. Commun.* **1985**, *26*, 81−83.
(39) (a) Popov, A. I.; Smitana, A. J.; Kintzinger, J.-P.; Nguyen, T. T. T. *Helv. Chim. Acta* **1980**, *63*, 668−673. (b) Fedarko, M.-C. *J. Magn. Reson.* **1973**, *12*, 30−35.
(40) Mehring, M. *Principles of High-Resolution NMR in Solids*, 2nd ed.; Springer-Verlag: New York, 1983.
(41) Schaefer, J.; Stejskel, E. O.; Buchdahl, R. *Macromolecules* **1977**, *10*, 384.
(42) Schaefer, J.; Stejskel, E. O.; Steger, T. R.; Sefcik, M. D.; Mckay, R. A. *Macromolecules* **1980**, *13*, 1121.
(43) VanderHart, D. L.; Garroway, A. N. *J. Chem. Phys.* **1979**, *71*, 2773.
(44) Okamoto, D. T.; Cooper, S. L.; T. W. Root, *Macromolecules* **1992**, *25*, 1068.
(45) Abragam, A. *The Principle of Nuclear Magnetism*; Oxford University Press: Oxford, England, 1961.

MA001096K